Surface Chemistry of SO_2 on Zn and ZnO: Photoemission and Molecular Orbital Studies

Sanjay Chaturvedi, José A. Rodriguez,* Tomas Jirsak, and Jan Hrbek

Department of Chemistry, Brookhaven National Laboratory, Upton, New York 11973

Received: May 18, 1998; In Final Form: July 13, 1998

The reaction of SO_2 with polycrystalline Zn and ZnO surfaces has been investigated using synchrotron-based high-resolution photoemission spectroscopy and ab initio self-consistent-field calculations. The chemistry of SO_2 on Zn surfaces is quite complex and depends on both the temperature of adsorption and the SO_2 exposure. At 300 K, SO_2 dissociates on a clean Zn surface to form atomic sulfur and atomic oxygen ($SO_{2,gas} \rightarrow S_a + 2O_a$; $SO_{2,gas} \rightarrow SO_{gas} + O_a$). The Zn ↔ SO_2 bonding interactions induce a significant weakening of the S−O bonds. The theoretical calculations suggest the η^2-O,O and η^2-S,O bonding conformations of SO_2 as the two possible precursors for the dissociation of the molecule. The dissociation reactions are much more exothermic than the formation of SO_3 or SO_4: $SO_{2,gas} + nO_a \rightarrow SO_x$, where $x = 3$ or 4. At high SO_2 exposures (300 K), when most surface sites are blocked and dissociation of SO_2 cannot occur, SO_3 and SO_4 are formed on the Zn surface. Adsorption at 100 K suppresses the SO_2 dissociation completely, and SO_3 is formed through the disproportionation reaction $2SO_{2,a} \rightarrow SO_{gas} + SO_{3,a}$. Zn shows a much higher reactivity toward SO_2 than late transition metals. All the results for the reaction of SO_2 with ZnO surfaces indicate oxygen to be the active site. The Zn−O bonds in ZnO substantially reduce the electron density of zinc, the metal centers become poor electron donors for π-back-donation into the LUMO of SO_2, and the molecule mostly bonds to the oxygen sites of the oxide surface. Dosing SO_2 on ZnO at 300 K results in the formation of surface SO_4 species, which are stable to temperatures above 500 K. Results from the ab initio SCF calculations indicate that SO_2 adsorbs on an oxygen site to form SO_3, which then reacts with a lattice oxygen atom to form SO_4. The last step in this process has a substantial activation energy, and after dosing SO_2 to ZnO at 100 K a mixture of SO_3 and SO_4 is produced on the surface.

I. Introduction

The interactions of sulfur with metal and oxide surfaces are of broad technological significance in the areas of catalyst poisoning, solar energy, and corrosion.[1−4] The role of sulfur oxides as air pollutants[5−10] and components of industrial processes[10] has spawned much interest in the surface chemistry of these compounds, particularly SO_2. Metal oxides offer a potential route for the removal or destruction of sulfur oxides. In several petrochemical processes, to prevent catalyst poisoning, sulfur compounds are removed from the feedstream by adsorption on a bed of ZnO.[11] In this article, we study the reaction of SO_2 with Zn and ZnO using synchrotron-based high-resolution photoemission and ab initio self-consistent-field (SCF) calculations.

Several recent studies have focused their attention on the interaction of SO_2 with metal single crystals such as Cu(111),[12−14] Cu(100),[14−18] Ag(111),[19−22] Ag(110),[8,22−24] Ag(100),[25−26] Pt(111),[27−35] Pt(100),[35] Pt(110),[36] Ni(110),[37−39] Ni(111),[40−42] Ni(100),[41−43] Pd(100),[44] and Zn(0001).[45] There is also some literature available for the reaction of SO_2 with polycrystalline Ni, Ag, Zn, Cd, and Cu.[46] Most of the studies have concentrated on the question of molecular versus dissociative adsorption and on the identification of adsorbed SO_x species resulting from the dissociation of SO_2. Generally, SO_2 adsorbs dissociatively on most metals (Cu, Pt, Ni, Pd, Fe, Rh, W, and Zn), except on Ag, where SO_2 adsorbs and desorbs molecularly.[47] Results from an earlier Auger electron spectroscopy study of SO_2/Zn(0001) showed the presence of at least two types of sulfur species.[45] The study, however, did not attempt to assign the exact nature of the sulfur species. A UV photoelectron spectroscopy study done much later suggested the formation of SO_3 or SO_4 species on polycrystalline Zn after reaction with SO_2 at room temperature.[46] In this paper, we present detailed results for the reaction of SO_2 with polycrystalline Zn at 100 and 300 K. The surface chemistry of SO_2 on Zn is very complex, and we have identified four sulfur species (S, SO_2, SO_3, and SO_4) whose presence is dependent on both coverage and temperature.

There is relatively little literature available examining the interaction of SO_2 with well-defined surfaces of oxides. It is limited to the following substrates: TiO_2(110),[48,49] Ti_2O_3-(10$\bar{1}$2),[50] Fe_2O_3(0001),[51] V_2O_3(10$\bar{1}$2),[52] V_2O_5(001),[53] NiO-(100),[54] Al_2O_3,[55−57] and MgO(100).[58] In general, these systems exhibit a very low reactivity toward SO_2, and only when defect sites are present on the surface, does one see significant interactions between the metal oxide and the molecule. This paper examines the reaction of SO_2 with polycrystalline ZnO at 100 and 300 K. On zinc oxide, SO_2 interacts mainly with the oxygen sites of the surface and evidence is found for multiple sulfur species (S, SO_2, SO_3, and SO_4). This rich surface chemistry is compared and contrasted to that of SO_2 on metallic Zn.

II. Experimental Section

All the experiments were performed in a conventional ultrahigh vacuum (UHV) chamber at the U7A beamline of the National Synchrotron Light Source (NSLS) at Brookhaven National Laboratory. The beamline is equipped with a toroidal-

* To whom all correspondence should be addressed. E-mail: rodrigez@bnl.gov. Fax: 516-344-5815.

S1089-5647(98)02269-X CCC: $15.00
Published on Web 08/14/1998

spherical grating monochromator that can deliver photons ranging in energy from 200 to 1200 eV. The UHV chamber is fitted with a hemispherical electron energy analyzer with multichannel detection, instrumentation for low-energy electron diffraction (LEED), and a quadrupole mass spectrometer. In addition, the chamber also has a Mg Kα X-ray source for X-ray photoelectron spectroscopy (XPS). To enhance the surface sensitivity, the sample was positioned at an angle of 45° with respect to the analyzer. All the S 2p spectra for the Zn and ZnO systems were acquired using a photon energy of 260 eV, while all the Zn 2p and O 1s spectra were taken with unmonochromatized Mg Kα radiation. The binding energy (BE) scale in the spectra acquired using synchrotron radiation was calibrated by the position of the Fermi edge in the valence band, while the BE scale in the experiments using the X-ray source was established by setting the O 1s peak of pure ZnO at a binding energy of 530.5 eV.[59]

Thick films of Zn were vapor deposited on a Pt(111) substrate at 100 or 300 K. The evaporation of Zn was achieved by heating a W filament wrapped with ultrapure Zn wire. The formation of Zn multilayers was confirmed by the complete disappearance of the Pt XPS signal. ZnO films (>10 monolayers (ML) thick) were grown on the clean Pt(111) crystal using procedures described elsewhere.[59−61] Following this methodology, one gets quasi-layer-by-layer growth and the ZnO films are polycrystalline with electronic properties and a phonon structure that are identical to those of bulk zinc oxide.[60,61] The polycrystalline Zn and ZnO surfaces were exposed to high-purity SO_2 gas (Mattheson) by backfilling the chamber at a certain pressure for a fixed period of time to get the desired coverage. The purity of the SO_2 gas was confirmed using a mass spectrometer. The coverage of sulfur on the surface (θ_S) was determined by measuring the area under the S 2p peaks, which was scaled to absolute units by comparing it to the corresponding area for 0.33 ML of S on Pt(111).[62]

III. Experimental Results

III.1. Reaction of SO_2 with Zn. Figure 1 shows S 2p spectra taken after exposing polycrystalline Zn to SO_2 at 300 K. At the lower SO_2 doses (up to 0.9 langmuir), the S 2p spectra exhibit a broad doublet between 161.5 and 163.5 eV. This is assigned to the presence of chemisorbed S on the Zn surface[59,63] and indicates that the SO_2 adsorption is dissociative at 300 K ($SO_{2,gas} \rightarrow S_a + 2O_a$). This argument is further supported by the O 1s data presented in the bottom panel of Figure 2, which will be discussed later in this section. At an SO_2 dose of 1.9 langmuirs ($\theta_S \approx 0.2$ ML), the S 2p spectrum shows the characteristic doublet for chemisorbed S on Zn and weak broad features between 164.5 and 168.5 eV start to appear. As the SO_2 dose is increased to 7.0 langmuirs, the S 2p spectra exhibits a very complex line shape that is comprised of multiple sulfur species. The single doublet with the S $2p_{3/2}$ peak centered at ∼162.5 eV is attributed to the presence of chemisorbed S on the surface.[59,63] The broad features between 164.5 and 169.5 eV are well fitted by three doublets. To assign these features, we used binding energies reported for sulfites and sulfates.[64] The main peak at 166.8 eV can be assigned to SO_3.[64] The two minor contributions can be attributed to SO_2 (S $2p_{3/2}$ feature at 165.8 eV) and a SO_4-like species (S $2p_{3/2}$ feature at 167.7 eV). The SO_3 and SO_4 species are probably produced by the reaction of SO_2 with chemisorbed oxygen atoms.[47] Additional SO_2 exposure further enhances the signal of these molecular features, and a total 12.0 langmuir dose results in a sulfur coverage (determined by measuring the total area under the S 2p peaks,

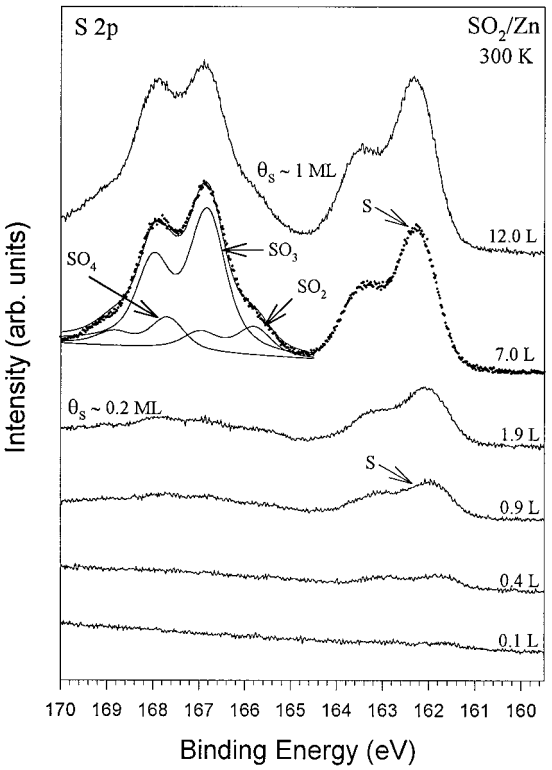

Figure 1. S 2p spectra for SO_2 dosed on a thick (>10 ML) polycrystalline Zn film at 300 K as a function of SO_2 exposure. All spectra were acquired using a photon energy of 260 eV.

see section II) that corresponds to ∼1.0 ML. At this point, the large sulfur and oxygen coverages suggest the presence of S, O, and SO_x species in the subsurface region.

The top panel of Figure 2 shows the valence band spectra recorded after dosing SO_2 to the polycrystalline Zn film. The bottom spectrum in this top panel corresponds to clean Zn and shows the Zn 3d band at ∼10 eV.[64b] At a 12.0 langmuir SO_2 dose, there is a complete change in the Zn 3d line shape and the main peak is centered at a binding energy of ∼11.0 eV, which indicates the oxidation of Zn and arises from the formation of $ZnSO_x$ and ZnO.[59] O 1s spectra for these experiments are shown in the bottom panel of Figure 2. A 0.4 langmuir SO_2 dose results in a small O 1s peak at ∼530.5 eV, probably due to the presence of chemisorbed oxygen on Zn since the S 2p data presented in Figure 1 showed no SO_x species at these coverages. It is worth noting that the amount of adsorbed oxygen produced after dosing 0.4 langmuir of SO_2 is more than double the amount of adsorbed sulfur. It is likely that a fraction of the dosed SO_2 partially decomposed on the surface ($SO_{2,gas} \rightarrow SO_{gas} + O_a$), producing no S adatoms. A 12.0 langmuir SO_2 dose at 300 K results in a O 1s line shape that is comprised of at least two distinct peaks. The feature at low binding energy (∼530.5 eV) is ascribed to O/Zn or ZnO[59] while the peak at ∼531.5 eV is due to $ZnSO_x$.[64a]

The surface chemistry of SO_2 adsorbed on polycrystalline Zn is strongly dependent on the adsorption temperature. Figures 3, 4, and 5 present the results for the reaction of SO_2 with polycrystalline Zn at 100 K. The top panel of Figure 3 presents the corresponding S 2p spectra as a function of SO_2 exposure. At the lowest SO_2 dose (0.1 langmuir), there is evidence only for the presence of chemisorbed molecular SO_2. At 100 K, there is limited mobility of SO_2 and the lack of $SO_2 \leftrightarrow SO_2$ interactions (due to the low coverage) prevents a disproportionation reaction. The S 2p line shape at a dose of 0.4 langmuir can be fitted with two doublets. The feature with the S $2p_{3/2}$

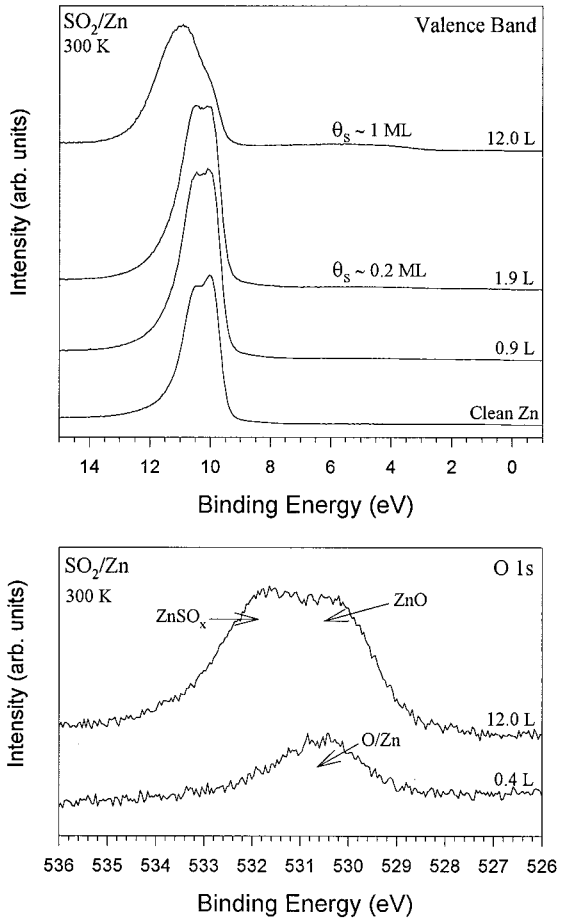

Figure 2. Top panel shows valence band spectra for SO_2/Zn at 300 K as a function of SO_2 exposures as indicated in the figure; all the spectra were acquired using a photon energy of 260 eV. Bottom panel shows O 1s spectra for 0.4 and 12.0 langmuir SO_2 dosed on Zn at 300 K. All the O 1s spectra were acquired using Mg Kα radiation.

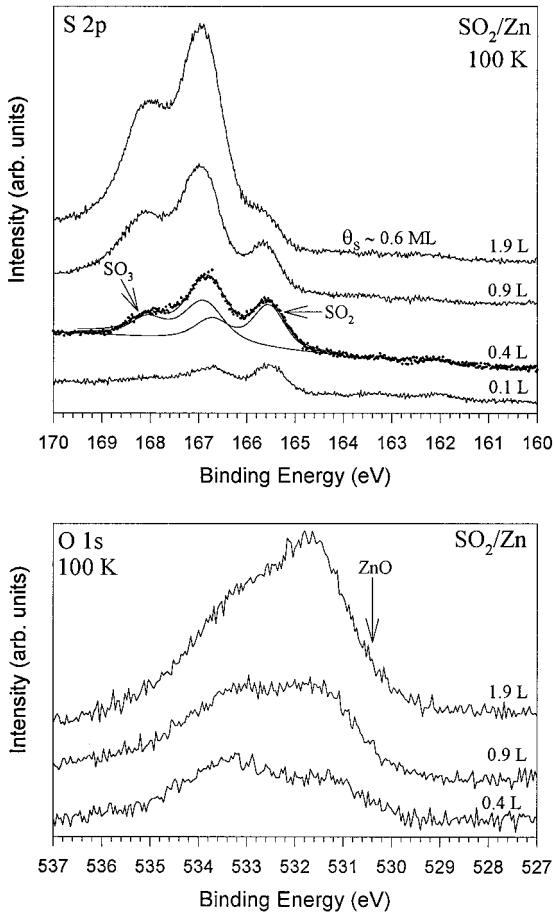

Figure 3. Top panel shows S 2p spectra for SO_2 dosed on a thick (>10 ML) polycrystalline Zn film at 100 K as a function of SO_2 exposure. All the S 2p spectra were acquired using a photon energy of 260 eV. Bottom panel shows O 1s spectra for 0.4, 0.9, and 1.9 langmuir SO_2 dosed on Zn at 100 K. All the O 1s spectra were acquired using Mg Kα radiation. The arrow at ~530.5 eV represents the peak position for ZnO.

level at ~165.5 eV is ascribed to SO_2, and the one with the S $2p_{3/2}$ level at ~166.9 eV is probably due to the formation of SO_3.[64] No signal is observed for chemisorbed atomic S. Thus, the SO_3 is being produced by a disproportionation reaction: $2SO_{2,a} \rightarrow SO_{gas} + SO_{3,a}$. As the SO_2 exposure is further increased to 1.9 langmuir ($\theta_S \approx 0.6$ ML), the amount of SO_3 adsorbed on the Zn surface increases, while the amount of SO_2 remains relatively constant. These observations are also supported by the O 1s data presented in the bottom panel of Figure 3. At a SO_2 exposure corresponding to 0.4 langmuir, the O 1s spectrum shows a broad feature with at least two components. The low binding energy feature at ~531.5 eV grows with increasing SO_2 exposure and is attributed to the formation of $ZnSO_3$ on the surface (see bottom panel in Figure 2). On the basis of the growth pattern of the two features, we tentatively assign the peak at ~533.4 eV to the presence of surface SO_2. One important observation is the complete absence of any peak at ~530.5 eV (see arrow in Figure 3), characteristic of the presence of chemisorbed oxygen on Zn or the formation of ZnO. This result is consistent with the S 2p data presented in the top panel, which does not show any evidence for the presence of atomic sulfur. Thus, the formed SO_3 is the product of disproportionation of SO_2 at 100 K. SO_2 disproportionation is not a major reaction channel in the experiments of Figure 1, because at room temperature, the concentration of adsorbed SO_2 is not large enough to allow this process to occur. At small SO_2 doses, the molecule dissociates, and at large SO_2 doses, the probability for $SO_{2,a} \leftrightarrow O_a$ interactions is much larger than the probability for $SO_{2,a} \leftrightarrow SO_{2,a}$ interactions.

The experiments in Figure 4 examine the thermal stability of sulfur oxides on zinc at temperatures between 100 and 300 K. The bottom spectrum in the panel corresponds to a SO_2 multilayer deposited at 100 K, and it shows the S $2p_{3/2}$ feature centered at ~169 eV. This is fairly consistent with the value reported for the SO_2 multilayer on Au (168.4 eV).[65] Annealing to 150 K removes this multilayer and produces a S 2p spectrum with a dominant S $2p_{3/2}$ feature centered at ~166.9 eV, which corresponds to the formation of surface SO_3 species (see Figure 1).[64] At this point, there is a lot of sulfur in the system, and using the area under the S 2p peaks, we estimate θ_S (see section II) to be at least 1.6 ML. Further annealing to 200 K reduces the intensity of this SO_3 feature and in addition results in the appearance of a well-defined doublet with the S $2p_{3/2}$ centered at ~162.4 eV. This feature is associated with chemisorbed sulfur (or ZnS) produced by the decomposition of adsorbed SO_3. Studies done on other transition-metal surfaces have shown that surface SO_x species start to decompose and form atomic sulfur at temperatures above 180 K.[27,47] Heating to 300 K causes little change in the total S 2p peak intensity ($\theta_S \approx 1.3$ ML) and simply results in an enhanced production of atomic sulfur accompanied by the decomposition of adsorbed SO_3. This final system is quite similar to that obtained by dosing SO_2 on polycrystalline Zn at 300 K (see Figure 1).

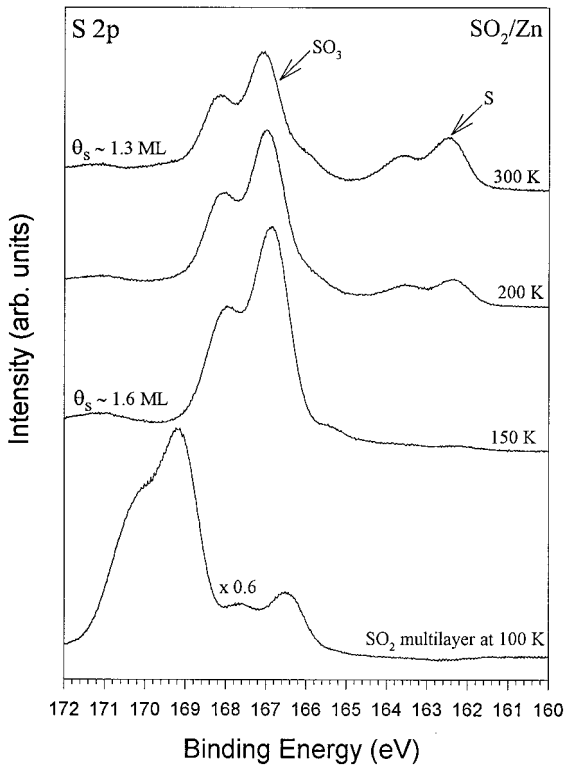

Figure 4. S 2p spectra for a SO_2 multilayer deposited on Zn at 100 K and subsequently annealed to temperatures indicated in the figure. All spectra were acquired using a photon energy of 260 eV.

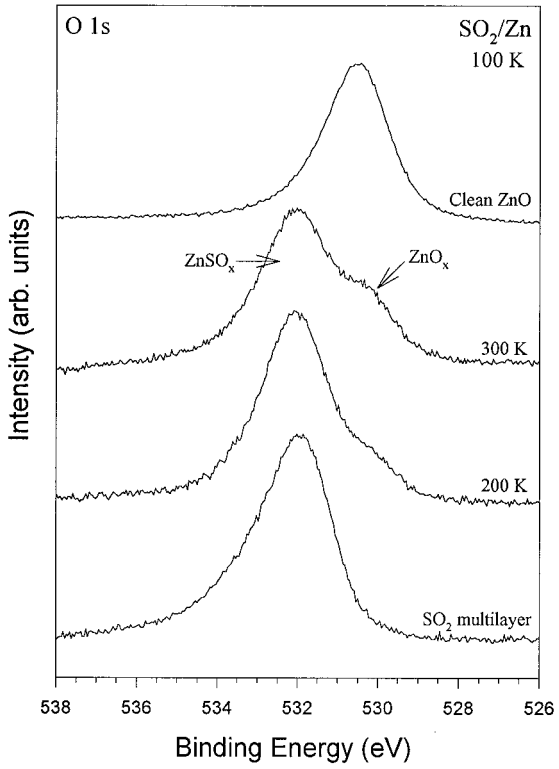

Figure 5. O 1s spectra for a SO_2 multilayer deposited on Zn at 100 K and subsequently annealed to temperatures indicated in the figure. The O 1s spectrum for clean ZnO is given at the top for reference. All the O 1s spectra were acquired using Mg Kα radiation.

The corresponding O 1s data for the experiment described in Figure 4 are shown in Figure 5. The spectrum for clean ZnO is shown at the top for reference. The SO_2 multilayer shows a peak at ~532 eV consistent with the values obtained previously for the SO_2 multilayer on Pt(111),[30] Ni,[65] and Au.[65] Annealing to 200 K causes the desorption of the physisorbed SO_2 (see Figure 4) and results in the appearance of a small shoulder at ~530.5 eV. This shoulder becomes more well defined upon annealing to 300 K, and we have two components in the O 1s spectrum: a high binding energy feature at ~532 eV ($ZnSO_x$) and another at ~530.5 (ZnO_x). Note once again that the final system obtained after dosing SO_2 on Zn at 100 K and annealing to 300 K is similar to the one obtained by dosing SO_2 at 300 K (bottom of Figure 2).

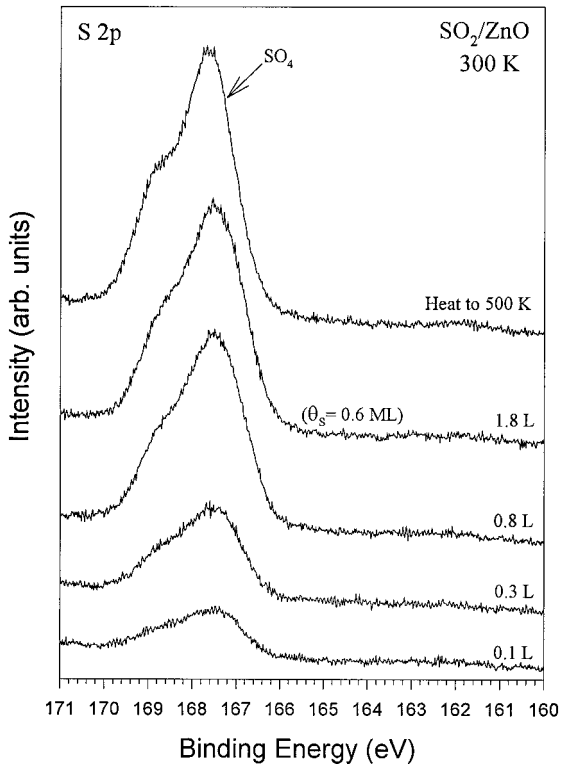

Figure 6. S 2p core level spectra for the SO_2/ZnO system as a function of SO_2 exposure. SO_2 was dosed at 300 K, and in the final step the surface was annealed to 500 K. All spectra were acquired using a photon energy of 260 eV.

III.2. Reaction of SO_2 with ZnO. In this section, we examine the adsorption of SO_2 on polycrystalline ZnO at 300 and 100 K. The type of oxide surfaces used in this study exposed approximately a 50:50 mixture of Zn and O.[61] Our previous studies have shown that the Zn sites of these surfaces are reactive toward S-containing molecules.[59,66] Figure 6 shows the S 2p spectra obtained after successive doses of SO_2 on ZnO at 300 K. Even at the lowest SO_2 exposures, we get a broad feature centered at ~167.5 eV, which we assign to the formation of a SO_4-like species (see Figure 1).[64,67] This feature grows in intensity with increasing SO_2 exposure. On pure Zn, where atomic S is the dominant species at 300 K and low exposures (<1.0 langmuir), SO_3 starts to form only at much higher SO_2 doses. This difference is probably due to the participation of lattice oxygen from ZnO. In fact, these results show that SO_2 preferentially reacts with O sites of the oxide and more or less ignores the Zn sites (the formed SO_4, however, does interact with the Zn sites). After an SO_2 exposure of 1.8 langmuir, the ZnO is covered with a SO_4 layer that has a sulfur coverage of ~0.6 ML. When the system was annealed to 500 K, the S 2p peaks became more well defined without any appreciable change in intensity. Most of the SO_4-like species disappeared after heating to 700 K, leaving mainly chemisorbed S on the Zn sites of the oxide surface (not shown).

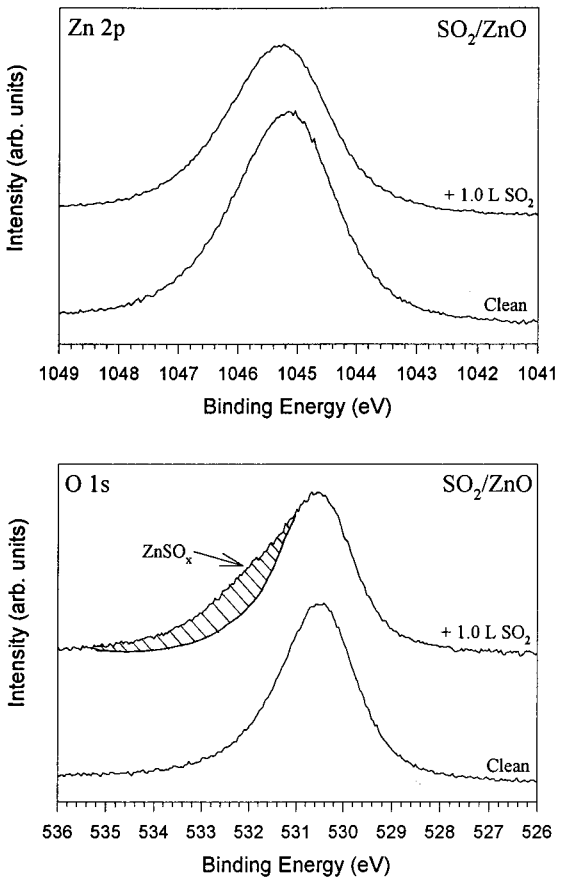

Figure 7. Top panel shows Zn $2p_{1/2}$ spectra of a clean and SO_2 dosed ZnO surface. SO_2 was dosed at 300 K. Bottom panel shows O 1s spectra for the experiment in the top panel. The hatched portion in the SO_2 dosed spectrum is due to the formation of $ZnSO_x$. All spectra were acquired using Mg Kα radiation.

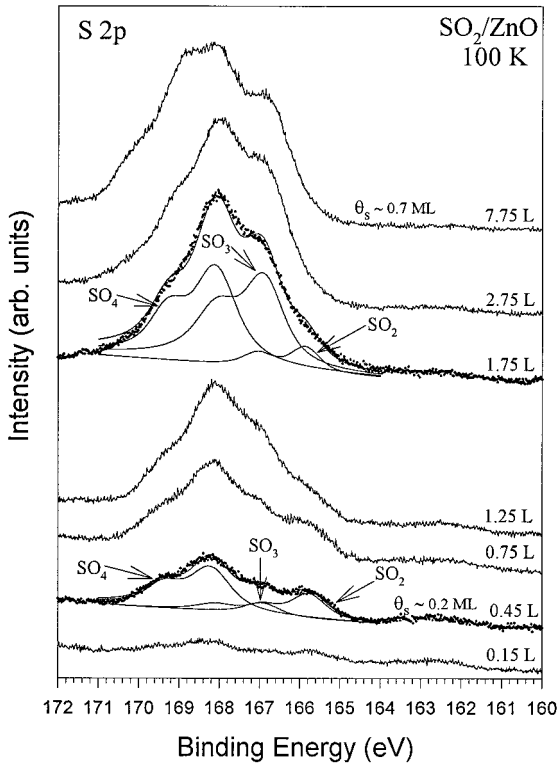

Figure 8. S 2p core level spectra for the SO_2/ZnO system as a function of SO_2 exposure at 100 K. The complex line shape indicates that there is a mixture of SO_x species. All spectra were acquired using a photon energy of 260 eV.

The top panel of Figure 7 shows the Zn $2p_{1/2}$ core level of ZnO both before and after reaction with SO_2. Clean ZnO exhibits a Zn $2p_{1/2}$ peak at 1045.0 eV,[59] and upon dosing 1.0 langmuir of SO_2 at 300 K, there is an attenuation in the Zn $2p_{1/2}$ signal and the peak shifts to 1045.2 eV. A more drastic change is seen in the corresponding O 1s data shown in the bottom panel of Figure 7. It can be clearly seen that the dosing of SO_2 introduces significant asymmetry in the O 1s spectrum toward the higher binding energy side. The hatched portion in the top spectrum of the bottom panel represents the contribution of the $ZnSO_x$ that is formed.

The results presented in the previous section indicate that the surface chemistry of SO_2 on Zn depends on the adsorption temperature. We decided to investigate if the same was also true for ZnO. Figure 8 presents S 2p spectra for the SO_2/ZnO system at 100 K as a function of SO_2 exposure. At the lowest SO_2 dose of 0.15 langmuir, weak features start to appear between 165 and 170 eV. These features grow in intensity as the exposure is increased to 0.45 langmuir. At this point, the sulfur coverage is estimated to be ~0.2 ML and the S 2p spectrum can be fitted with three doublets. The one with the S $2p_{3/2}$ centered at 165.8 eV is assigned to SO_2 bonded to Zn sites. A similar feature is also obtained when SO_2 is dosed on pure Zn at 100 K. The other major doublet has a S $2p_{3/2}$ peak centered at 168.2 eV, and this is assigned to the presence of surface SO_4.[64] Since we do not see any evidence for peaks at ~162 eV that would correspond to atomic sulfur, it is valid to conclude that the surface SO_4 that is formed is a result of the reaction of SO_2 with surface oxygen from ZnO. There is also evidence for a small amount of surface SO_3 (doublet with S $2p_{3/2}$ centered at 166.8 eV).[64] As the SO_2 exposure is increased, the amount of SO_2 remains relatively constant while there is a significant increase in the amount of SO_3 and SO_4. At an exposure corresponding to 1.75 langmuir, there is an almost equal amount of surface SO_3 and SO_4. An additional SO_2 dose results in a further increase in the intensity of these features, and it is possible to get a sulfur coverage as high as ~0.7 ML upon dosing 7.75 langmuir of SO_2. From all these observations, it appears that at 100 K there is formation of both SO_3 and SO_4, while at 300 K the only dominant reaction channel is the formation of SO_4. It seems that higher temperatures are required to drive the complete oxidation of surface SO_2 to SO_4. This is presumably because higher thermal energy facilitates the reconstruction of ZnO that makes oxygen available for the formation of SO_4-type species.

Shown in Figure 9 are S 2p spectra that were acquired after heating a ZnO surface that was saturated with SO_2 at 100 K. The SO_2 multilayer exhibits a similar line shape to that of a SO_2 multilayer on pure Zn (see Figure 4). There is a loss of the SO_2 multilayer and multiple features appear between 166 and 170 eV upon annealing to 150 K. By use of the S 2p area, the sulfur coverage at this point is estimated to be ~1.0 ML (i.e., the SO_x groups are not confined to the surface of the system), and the S 2p line shape indicates the existence of at least two sulfur species (probably SO_3 and SO_4). Annealing to 300 K results in significant losses in the peak intensities, indicating that there is some desorption of sulfur probably as SO_2. In addition, a weak doublet starts to grow at ~162 eV, which corresponds to the presence of sulfur chemisorbed on zinc, and this suggests that a small fraction of the surface SO_x species decompose to form atomic sulfur. This behavior becomes more evident as the sample is annealed to 500 K. The total areas under the S 2p spectra for 300 and 500 K are quite

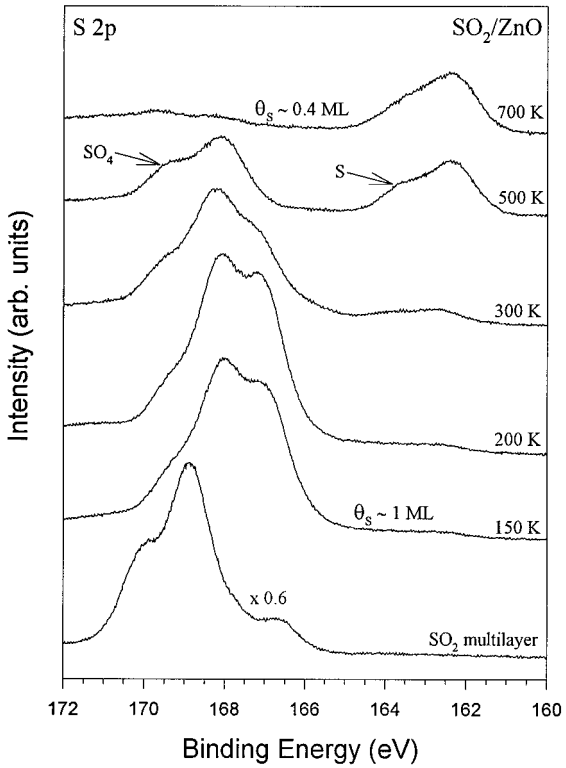

Figure 9. S 2p spectra for a SO_2 multilayer deposited on ZnO at 100 K and subsequently annealed to temperatures indicated in the figure. Annealing to 150 K desorbs the multilayer and results in a sulfur coverage equal to ~1 ML. Annealing to 500 K results in a mixture of SO_x and atomic S on the surface, and further annealing to 700 K partially transforms the SO_x to atomic sulfur. All spectra were acquired using a photon energy of 260 eV.

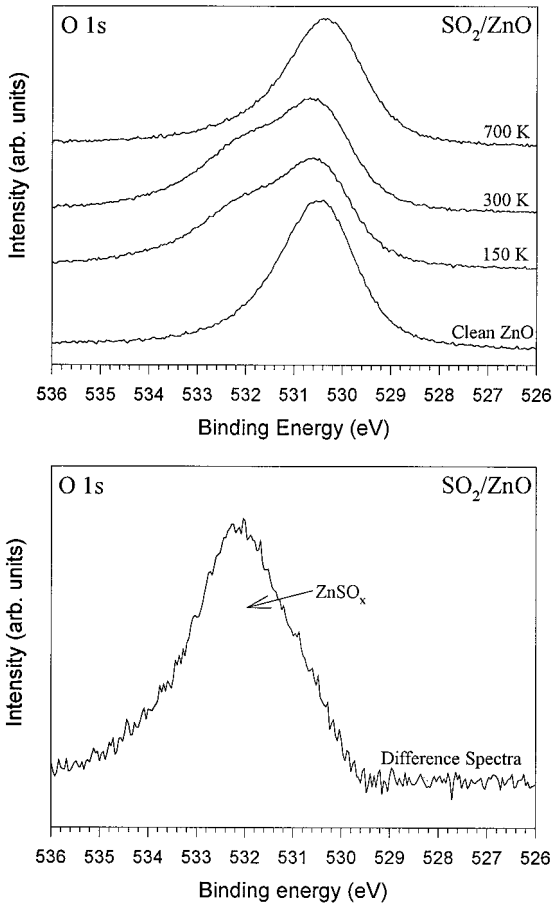

Figure 10. Top panel shows O 1s spectra for clean and SO_2-dosed ZnO surfaces. The spectra were recorded after dosing a SO_2 multilayer on ZnO at 100 K and subsequently annealing to the temperatures indicated in the figure. Bottom panel shows a difference spectrum of the 300 K and clean ZnO spectrum from the top panel. The clean ZnO spectrum was normalized to the intensity of the 300 K spectrum at 530.5 eV.

comparable. Also, the doublet with the S $2p_{3/2}$ level centered at ~166.5 eV, assigned to SO_3,[64] has disappeared, and the only SO_x species left on the surface is SO_4. Formation of ZnS at this elevated temperature cannot be ruled out. Further annealing to 700 K results in an almost complete loss of the SO_4, and the resulting peak area of Zn-bonded S (θ_S = 0.4 ML) suggests that at least part of the SO_4 may have converted into this species.

The S 2p spectra presented in Figure 9 indicate that upon dosing SO_2 on ZnO, $ZnSO_x$ is formed at temperatures between 150 and 500 K and at higher temperatures (700 K) it decomposes to form Zn-bonded S and probably gaseous SO_2. The formation and stability of $ZnSO_x$ are further substantiated by the O 1s data presented in Figure 10. The bottom spectrum in the top panel of Figure 10 shows the O 1s core level of clean ZnO. Upon dosing SO_2 at 100 K and annealing to 150 K, to remove the SO_2 multilayer, there is a large asymmetry introduced in the O 1s line shape toward the higher binding energy side. This asymmetry becomes more well defined as the sample is heated to 300 K. The bottom panel of Figure 10 shows the difference spectrum obtained after subtracting the clean ZnO spectrum from the one corresponding to 300 K (the clean ZnO spectrum was normalized to the intensity of the 300 K spectrum at 530.5 eV). This allows a clear assignment of the peak at ~532 eV to the formation of $ZnSO_x$. This is similar to the result obtained for the SO_2/Zn system (see Figure 5) where one sees the formation of both $ZnSO_x$ and ZnO. Annealing to 700 K causes the high binding energy feature at ~532 eV to disappear, and this is consistent with the decomposition of $ZnSO_x$ seen in Figure 9.

IV. Theoretical Results

IV.1. Bonding Interactions of SO_2 and SO_3 with Zn(0001). The photoemission data shown in section III.1 indicate that SO_2 adsorbs molecularly on polycrystalline Zn at 100 K. At room temperature, the molecule decomposes ($SO_2 \rightarrow S + 2O$) or reacts with oxygen adatoms to form SO_3. In this section, we use ab initio SCF calculations to investigate the bonding interactions between SO_2 and the (0001) face of Zn (the most common type of terrace seen in polycrystalline Zn[60]). The Zn-(0001) surface was modeled using the cluster shown at the top of Figure 11. This metal cluster contains 15 atoms arranged in two layers with the geometry reported for bulk Zn.[68] The molecular orbital (MO) calculations reported in this paper were performed using the HONDO program.[69] Since the systems under consideration contain a large number of heavy atoms, the nonempirical effective core potential of Hay and Wadt was used to describe the inner shells of zinc.[70] A basis set obtained through a (3s3p5d/2s1p2d) contraction scheme[59,60,66,71] was used to describe the 4s, 4p, and 3d valence orbitals of zinc. The atomic orbitals of sulfur and oxygen were expressed in terms of double-ζ quality basis sets augmented with polarization functions.[59,60,66,68,72]

Figure 12 shows the bonding configurations of SO_2 when the molecule was adsorbed on a-top and bridge sites of cluster I. SO_2 adopts these bonding conformations in inorganic complexes[73,74] and on metal surfaces.[47,75] In our adsorption

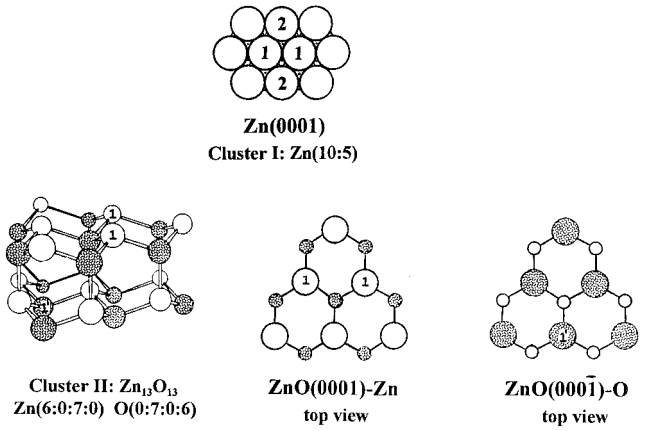

Figure 11. Cluster used to model the Zn(0001) surface (top). The clusters have 15 atoms arranged in two layers. The (·) dots indicate 3-fold hollow sites that have a Zn atom underneath in the second layer. SO_2 and SO_3 were adsorbed on the Zn atoms labeled 1. Top and side views of the cluster used to model the (0001)−Zn and (000$\bar{1}$)−O faces of zinc oxide (bottom). The cluster has 13 zinc atoms (empty circles) and 13 oxygen atoms (shaded circles) arranged in four layers. The notation (a:b:c:d) specifies how many Zn (or O) atoms are in each layer. The (0001)−Zn and (000$\bar{1}$)−O faces of ZnO are represented by the first and fourth layers, respectively. The SO_2 molecule was adsorbed on the Zn atoms labeled 1 or on the O atom labeled 1′.

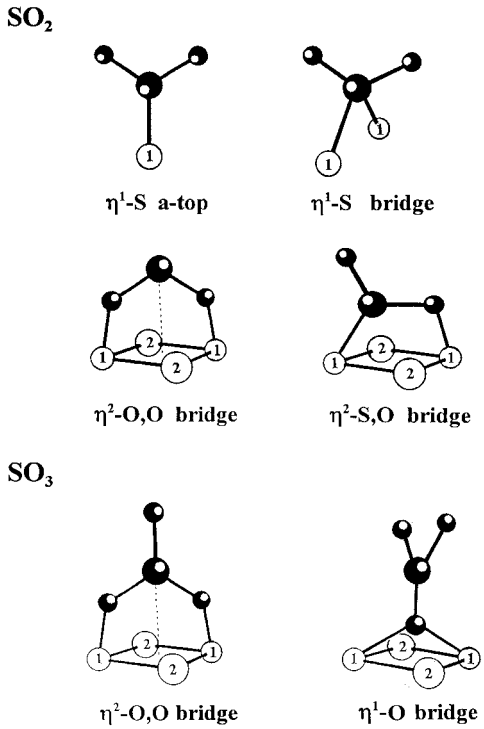

Figure 12. Bonding configurations for SO_2 (top) and SO_3 (bottom) on Zn(0001). The molecules were adsorbed with their molecular planes perpendicular to the surface. The empty circles labeled 1 and 2 represent zinc atoms of cluster I (see Figure 11).

models, we kept the molecular plane of SO_2 perpendicular to the Zn(0001) surface, as proposed in previous theoretical and experimental studies for the adsorption of SO_2 on metals.[24,30,44,75−76] Table 1 lists the optimal values given by the SCF calculations for the structural parameters of adsorbed SO_2. For the free SO_2 molecule, the calculated S−O bond distances (1.42 Å) and O−S−O bond angle (118°) are very close to the reported experimental values (1.43 Å and 119°).[47] The changes induced by chemisorption on the geometry of SO_2 are similar to those seen after bonding the molecule to metals

TABLE 1: Adsorption of SO_2 on Zinc

	geometry				adsorption energy (kcal/mol)[a]
	Zn_1-S (Å)	Zn_1-O (Å)	S−O (Å)	O−S−O (deg)	
free SO_2			1.42	118	
on Zn (0001)					
η^1−S a-top	2.36		1.43	118	7
η^1−S bridge	2.39		1.45	118	11
η^2−O,O bridge		2.08	1.49	122	16
η^2−O,S bridge	2.40	2.11	1.51	121	14
			(1.44)[b]		

[a] Positive values denote an exothermic process. [b] Oxygen atom nonbonded to zinc.

in inorganic complexes.[73,74] The predicted Zn−S (2.36−2.40 Å) and Zn−O (2.08−2.11 Å) bond lengths are within the range of distances observed in X-ray diffraction studies for Zn−S and Zn−O bonds in inorganic compounds.[74−77] In principle, the bonding mechanism of SO_2 to a metal or oxide can involve donation of electrons from the occupied σ ($8a_1$,$5b_2$) or π ($1a_2$) orbitals of the molecule into the surface, plus a transfer of electrons from the metal or oxide into the empty $3b_1$ orbital (LUMO) of SO_2 (π-back-donation).[47,73] In Table 1, the increase in the length of the S−O bonds induced by chemisorption (0.02−0.09 Å) reflects a weakening in the strength of these bonds produced in part by a depopulation of the $8a_1$ orbital (slightly bonding between sulfur and oxygen) and a population of the $3b_1$ orbital (moderately antibonding between sulfur and oxygen) upon adsorption.

Table 1 shows bonding energies calculated for the interaction of SO_2 with cluster I. It is likely that the values listed in the table underestimate the adsorption energy of SO_2 on Zn(0001) due to the lack of electron correlation in our calculations.[78] When dealing with adsorption energies, we will focus our attention on qualitative trends. For the bonding configurations of Figure 12, the strength of the Zn−SO_2 adsorption bond increases in the following sequence: η^1-S a-top < η^1-S bridge < η^2-S,O bridge ≈ η^2-O,O bridge. SO_2 bonded to a single Zn atom through its S end exhibits the weakest adsorption bond and the smallest perturbations in the S−O bonds. Thus, in this bonding conformation, the molecule is not expected to dissociate. For the η^2-O,O and η^2-S,O coordinations, the strength of the bonding interactions with the Zn substrate is similar and the SCF results cannot be used to predict which of these configurations is more stable. These two bonding conformations are probably the precursors for the dissociation of the molecule on zinc surfaces.

SO_3 can be a product of the reaction between SO_2 gas and O adatoms. We examined the adsorption of SO_3 on Zn(0001) with the admolecule coordinated as shown in the bottom of Figure 12 or monocoordinated through O to a hollow site of the surface. These bonding configurations have been frequently proposed in previous studies that deal with the properties of adsorbed SO_3.[47,75−76] According to our SCF calculations, the strength of the Zn−SO_3 adsorption bond increases in the following sequence: η^1-O bridge < η^1-O hollow < η^2-O,O bridge (Table 2). Dicoordination via O,O is predicted as the most stable adsorption geometry. Free SO_3 is a planar molecule (D_{3h} group) in which the S−O bonds are all equivalent and have a length of 1.43 Å.[79] Chemisorption induces a small elongation (∼0.06 Å, Table 2) in the S−O bonds of the oxygen atoms that are bonded to the Zn surface.

When SO_2 is dosed to Zn, a molecule can adsorb and dissociate on the empty sites of the surface:

$$SO_{2,gas} \rightarrow S_a + 2O_a \qquad (1)$$

TABLE 2: Adsorption of SO_3 on Zinc

	geometry				adsorption energy (kcal/mol)
	Zn_1-O (Å)	$S-O_B$ (Å)[a]	$S-O_{NB}$ (Å)[a]	O_B-S-O_{NB} (deg)	
free SO_3		1.41	1.41	120	
on Zn (0001)					
η^1-O hollow	2.12	1.47	1.42	119	18
η^1-O bridge	2.08	1.48	1.43	118	17
η^2-O,O bridge	2.07	1.47	1.42	118	22

[a] Oxygen atoms bonded (B) or nonbonded (NB) to the Zn substrate.

or it can react with O adatoms produced by the previous dissociation of other molecules:

$$SO_{2,gas} + O_a \rightarrow SO_{3,a} \quad (2)$$

The energetics derived from the SCF calculations predicts that both chemical processes release energy, but reaction 1 is ~14 kcal/mol more exothermic than reaction 2. Thus, the formation of SO_3 should take place only when the number of empty adsorption sites is limited, and therefore, reaction 1 cannot occur. Indeed, this is consistent with the trends seen in Figure 1 for the reaction of SO_2 with zinc at 300 K. The SCF calculations also predict that the molecular adsorption of SO_2 is less exothermic than its dissociative adsorption. Again this prediction agrees well with the data in Figure 1, where SO_2 prefers to decompose on clean zinc at room temperature. However, at 100 K, SO_2 adsorbs molecularly (Figure 3). Although the chemisorption process weakens the S−O bonds in SO_2, there is still a substantial activation energy for the breaking of these bonds, and at low temperatures an isolated admolecule is not able to overcome this kinetic barrier.

The photoemission results in Figures 1 and 3 show that the S 2p core levels are very sensitive to the chemical environment around sulfur on a zinc surface. The large variations seen in the S 2p binding energies ($S < SO_2 < SO_3$) reflect changes in the initial state of the S 2p core levels. Our SCF calculations show that for a sulfur atom bonded to a hollow site of cluster I the S 2p electrons are ~8.1 eV less stable than those of SO_2 bonded in a η^2-O,O bridge configuration. On the other hand, the S 2p electrons of O,O dicoordinated SO_2 are ~2.7 eV less stable than the S 2p electrons of O,O dicoordinated SO_3. (These differences come from applying Koopmans' theorem and do not include effects of final-state relaxation that occur during the photoemission process[80]). The shifts in the S 2p levels track variations in the charge on S:[81] −0.6e for the sulfur adatom, +1.3e for S in adsorbed SO_2, and +1.8e for S in adsorbed SO_3.

IV.2. Bonding Interactions of SO_2 with ZnO(0001)−Zn and ZnO(000$\bar{1}$)−O. The experiments for the adsorption of SO_2 on polycrystalline ZnO indicate that the molecule mainly interacts with oxygen sites of this surface. In this section, we study the adsorption of SO_2 on ZnO(0001)−Zn and ZnO(000$\bar{1}$)−O at a molecular orbital level using ab initio SCF calculations. The (0001)−Zn and (000$\bar{1}$)−O faces of zinc oxide were modeled using the cluster shown at the bottom of Figure 11. Previous studies have shown that clusters of this size provide the basic physical and chemical interactions that are responsible for the bonding of small molecules to zinc oxide surfaces.[59,66,82] Cluster II has the same total number of Zn and O atoms (13) arranged in the geometry of bulk zinc oxide.[83] The first and third layers are entirely zinc, and the second and fourth layers are comprised of purely O atoms. The first layer is a model for the ZnO(000$\bar{1}$)−Zn surface, whereas the fourth layer represents the ZnO(000$\bar{1}$)−O surface. In the SCF calculations, the Zn atoms in cluster II ($Zn_{13}O_{13}$) were described in the same way used to describe the Zn atoms in cluster I (Zn_{15}). Most of the oxygen atoms were treated using the effective core potential (1s shell) and orbital basis set (2s,2p shells) recommended by Stevens−Basch−Krauss.[84] The only exception was the O atom labeled 1′ in the fourth layer (on which SO_2 was adsorbed; see below). For this O atom, we included all its electrons in the calculations and the atomic orbitals were expressed using the same basis set employed to describe the oxygens in the SO_2 molecule (see section IV.1).

TABLE 3: Adsorption of SO_2 on Zinc Oxide

	geometry				adsorption energy (kcal/mol)[b]
	X_1-S (Å)[a]	X_1-O (Å)[a]	S−O (Å)	O−S−O (deg)	
on ZnO (0001)−Zn					
η^1-S a-top	2.40		1.42	118	4
η^1-S bridge	2.42		1.44	118	5
η^2-O,O bridge		2.12	1.46	120	12
η^2-S,O bridge	2.43	2.14	1.45	118	7
On ZnO(000$\bar{1}$)−O					
η^1-S a-top	1.54		1.41	119	29

[a] $X_1 = Zn_1$ in the case of ZnO(0001)−Zn, and $X_1 = O_1$ in the case of ZnO(000$\bar{1}$)−O. [b] Positive values denote an exothermic process.

On the Zn-terminated face of cluster II, SO_2 was adsorbed with the bonding conformations shown in Figure 12 (on top of a Zn_1 atom or bridging the two Zn_1 atoms). In these systems, the adsorption process induced only minor changes in the geometry of SO_2 (see Table 3) and the Zn ↔ SO_2 bonding interactions were much weaker than those on a pure zinc cluster (compare adsorption energies in Tables 1 and 3). The Zn−O bonds reduce the electron density on zinc, making more difficult the donation of electrons from the metal into the LUMO of SO_2 (the so-called "π-back-donation"[47,73]). This electron transfer plays a very important role in the bonding interactions between SO_2 and metals.[73,85−87] In Table 3, dicoordination via O,O is the most stable adsorption geometry for SO_2 on ZnO(0001)−Zn.

SO_2 interacts very strongly with the O-terminated face of cluster II. On this face, the molecule was bonded via S to the O atom labeled 1′ (η^1-S a-top conformation in Figure 12). After this adsorption geometry is optimized, the molecular plane of SO_2 was perpendicular to the (000$\bar{1}$)−O surface. This bonding configuration produced a SO_3-like species, and the adsorption energy of the molecule was much larger than that on the (0001)−Zn face (see Table 3). This agrees with the experimental trends seen in Figures 6 and 8, where SO_2 mainly reacts with O sites of polycrystalline ZnO. In principle, the adsorption of SO_2 on ZnO(000$\bar{1}$)−O via sulfur bridging two oxygen atoms of the surface (similar to a η^1-S bridge conformation in Figure 12) produces a SO_4-like species. We investigated this adsorption geometry and found that it was much less stable than the coordination of the molecule to only one oxygen atom (formation of SO_3-like species). The problem here is that the O−O separation in an ideal ZnO(000$\bar{1}$)−O surface (3.25 Å[83,88]) is too large to allow the formation of a SO_4-like species with the structural parameters of the SO_4 molecule or ion.[74,89−90] The formation of a stable SO_4-like species requires a substantial reconstruction in the (000$\bar{1}$)−O surface. This reconstruction cannot be modeled using cluster II, but it can be expected in zinc oxide surfaces because $ZnSO_4$ ($\Delta H_f = -235$ kcal/mol[91]) is much more stable than ZnO ($\Delta H_f = -83$ kcal/mol[91]). Comparing the results of Figures 6 and 8, one finds that after dosing SO_2 to ZnO at 300 K only the formation of SO_4 takes place, whereas at 100 K a large amount of SO_3 is formed. At room temperature, the atoms in the ZnO lattice are mobile

enough to allow the surface reconstruction that is necessary for the formation of SO_4. On the other hand, at 100 K the reconstruction of the surface is more difficult, and one sees the formation of a species such as SO_3, which does not require substantial changes in the morphology of the system.

V. Discussion

V.1. Reaction of SO_2 with Metallic Zn. Results from an earlier Auger electron spectroscopy study of SO_2/Zn(0001) showed the presence of at least two types of sulfur species[45] between 165 and 295 K and suggested that the two species may represent atomic sulfur chemisorbed on top of Zn atoms or on hollow sites. Our results for experiments conducted at 100 and 300 K indicate that it is more likely that the two distinct sulfur species are actually sulfur atoms in different chemical environments. One is atomic sulfur bonded to Zn and the other is sulfur bonded to the Zn surface as SO_x. A UV photoelectron spectroscopy study attempted to address the exact nature of SO_x and suggested the formation of SO_3 or SO_4 species on polycrystalline Zn after reaction with SO_2 at room temperature.[46] Our S 2p spectra indicate that the major component of SO_x is SO_3.

The results presented in section III.1 clearly show that the surface chemistry of SO_2/Zn is quite complex and depends on the SO_2 exposure and the temperature of adsorption. At 300 K, below 0.9 langmuir doses, the adsorption of SO_2 is primarily dissociative and leads to the formation of chemisorbed atomic sulfur and oxygen on the Zn surface. This type of dissociative chemisorption has been observed in many other metal surfaces,[47,92−93] and is facilitated by a weakening induced on the S−O bonds by the $SO_2 \leftrightarrow$ metal bonding interactions (see section IV.1 and refs 75 and 76). It is only at higher exposures ($\geq$1.9 langmuir), once the Zn sites are substantially covered, that the SO_2 reacts with adsorbed O to form SO_3. This behavior is consistent with the energetics derived from the SCF calculations in section IV.1. At 100 K, adsorbed SO_2 does not have the activation energy necessary to overcome the kinetic barrier for full dissociation, and when the number of SO_2 molecules on the surface is large, one sees the formation of SO_3 through a disproportionation reaction ($2SO_{2,a} \rightarrow SO_{gas} + SO_{3,a}$). This chemistry is very interesting because late transition metals only chemisorb SO_2 molecularly at 100 K (i.e., no formation of SO_3 or SO_4).[47] The driving force for the SO_2 disproportionation on Zn is the very large stability of zinc sulfites.[91]

When compared to the late transition metals (Ni, Pd, Pt, Cu, Ag, and Au),[12−44] zinc shows an extremely high reactivity toward SO_2. On other metals, the reaction with SO_2 at 300 K produces saturation coverages of S, O, and SO_x species that are at the submonolayer level.[12−44] This is not the case on zinc, where total sulfur coverages well above a monolayer are relatively easy to produce (even at 150 K, see Figure 4) and the sulfur species penetrate into the bulk of the sample. SO_2 virtually corrodes metallic zinc under UHV conditions. This phenomenon is made possible by the combination of two factors. First, the thermochemical stability of zinc sulfites and sulfates is very large[91] and second, the cohesive energy of metallic zinc is so low (31 kcal/mol)[68] that the potential barrier for the penetration of S, O, and SO_x into the bulk of the metal is probably very small.

V.2. Reaction of SO_2 with ZnO. The reaction of SO_2 with ZnO is markedly different from its reaction with Zn. On ZnO, SO_2 preferentially reacts with the O sites of the surface. In the oxide, the Zn−O bonds substantially reduce the electron density of zinc, the metal centers become poor electron donors for π-back-donation into the LUMO of SO_2, and the molecule mostly bonds to the oxygen sites of the surface. Unlike on Zn, where the oxidation is usually terminated at the formation of surface SO_3, on ZnO, the availability of lattice oxygen facilitates complete oxidation all the way to the formation of surface SO_4. An inspection of the heats of formation of $ZnSO_4$ ($\Delta H_f = -235$ kcal/mol[91]) and ZnO ($\Delta H_f = -83$ kcal/mol[91]) reveals that complete oxidation to form $ZnSO_4$ is an energetically favorable process. The formation of surface SO_3/SO_4 has also been observed after adsorbing SO_2 on other oxide surfaces such as α-Fe_2O_3(0001),[51] TiO_2(110),[48−49] TiO_2(441),[49] V_2O_3(10$\bar{1}$2),[52] MgO(001),[58] and Al_2O_3.[55] SO_3/SO_4 species have been detected after dosing S_2 to ZnO[59] and Cu_2O[72] or after reacting H_2S at atmospheric pressures with $NiMoO_4$.[94]

In the case of SO_2/ZnO, it was already mentioned in section IV.2 that the O−O separation in ZnO (3.25 Å[83,88]) is too large to allow direct formation of SO_4-like species with the structural parameters of the SO_4 molecule or ion.[74,89,90] The SO_2 molecule probably attaches itself to a surface oxygen atom to form SO_3, and a subsequent reconstruction of the oxide surface produces SO_4. This type of "mechanism" has also been proposed for the formation of SO_4 on MgO.[86] On powders of γ-alumina,[57] sulfur dioxide chemisorbs initially at basic sites to form an adsorbed sulfite, which converts to sulfate upon heating to high temperature or exposure to O_2.

It is interesting to contrast the reactions of SO_2 and S_2 with ZnO. In an earlier study, we reported the formation of atomic sulfur chemisorbed on Zn when S_2 was dosed on ZnO at 300 K.[59] At high sulfur coverages (>0.4 ML), we also saw the formation of a small amount of SO_x species. These SO_x species represented less than 10% of all the sulfur present on the surface.[59] The S 2p binding energy positions of these peaks suggest that they correspond to SO_3 (i.e., no formation of surface SO_4). Essentially, all the chemistry was occurring on the metal (Zn) sites. In a similar way, when H_2S is dosed on polycrystalline ZnO,[66] ZnO(0001),[95] or ZnO(10$\bar{1}$0),[95] one sees complete decomposition of the molecule and the S atoms prefer to bond with the Zn sites instead of forming SO_3 or SO_4. It is kinetically difficult for a sulfur atom to remove three or four oxygen atoms from ZnO to form SO_3 or SO_4, whereas adsorption of SO_2 on ZnO easily produces SO_3 species that are the precursors for the formation of SO_4. Similarly, when S_2 or H_2S is dosed on alumina, there is absolutely no trace of formation of any SO_x species[72,96] and once again all the chemistry occurs on the metal (Al) sites. However, SO_2 on Al_2O_3 readily forms surface SO_3 and SO_4 species.[55,57] All these results together indicate that it is very difficult for a S adatom to abstract several oxygens from an oxide lattice to form sulfites or sulfates. In addition, the probability for the reaction between H_2S and O sites is very low, and only at atmospheric pressures one can see the production of SO_3 and SO_4 species.[94]

It is well-known that small amounts of SO_2 can poison many metal/oxide catalysts.[2−3,56] In these systems, an important issue is the thermal stability of the adsorbed SO_x species on the metal and oxide phases of the catalyst. In some cases, the effects of SO_2 poisoning can be alleviated by operating the catalyst at high temperature.[2,56b] Our experiments indicate that the SO_3/SO_4 species formed on ZnO are stable at temperatures well above 500 K. In contrast, on typical metals (Ni, Pd, Pt, Ru, and Cu), the SO_3/SO_4 species usually decompose at temperatures below 500 K.[14,27,30,37,44,47] Thus, in ZnO-based catalysts, the oxide phase is expected to be more sensitive to SO_2 poisoning than the metal phase.

VI. Conclusions

The results obtained for the SO_2/Zn and SO_2/ZnO systems can be briefly summarized as follows:

(1) At low exposures (<1.0 langmuir) and 300 K, the adsorption of SO_2 on Zn surfaces is dissociative: $SO_{2,gas} \rightarrow SO_{gas} + O_a$; $SO_{2,gas} \rightarrow S_a + 2O_a$. Chemisorption induces a significant weakening in the strength of the S−O bonds in SO_2. Theoretical calculations predict that η^2-O,O and η^2-S,O bonding conformations are probably the precursors for the dissociation of the molecule. The dissociation reactions are much more exothermic than the formation of SO_3 or SO_4: $SO_{2,gas} + nO_a \rightarrow SO_{(2+n),a}$, where $n = 1$ or 2. At high SO_2 doses (>2.0 langmuir), when most surface sites are blocked and dissociation of SO_2 cannot occur, SO_x species are formed on Zn and the primary component of these SO_x species is SO_3.

(2) SO_2 does not dissociate to form atomic sulfur or oxygen on Zn surfaces at 100 K. Under these conditions, adsorbed SO_2 undergoes a disproportionation reaction ($2SO_{2,ads} \rightarrow SO_{gas} + SO_{3,ads}$) not seen for late transition metals. Zinc exhibits an extremely high reactivity toward SO_2. The reaction with SO_2 at 100−150 K produces a multilayer of $ZnSO_3$ that partially decomposes into ZnO and ZnS upon annealing to 300 K.

(3) The chemistry of SO_2 on ZnO is complex, and oxygen is the active site. When SO_2 is dosed on ZnO at 100 K, a mixture of SO_3 and SO_4 species is formed on the surface. Theoretical calculations suggest that SO_2 adsorbs on an oxygen site to form SO_3, which later extracts an oxygen atom from the ZnO lattice to form SO_4. At 100 K, the energy available for this "extraction" is limited due to the low temperature of the system.

(4) SO_2 dosed on ZnO at 300 K forms surface SO_4 species that are stable up to temperatures above 500 K. These SO_4 species decompose to form Zn-bonded S and ZnO.

Acknowledgment. This work was carried out at Brookhaven National Laboratory under Contract DE-AC02-98CH10886 with the U.S. Department of Energy, Office of Basic Sciences, Chemical Science Division. The NSLS is supported by the divisions of Materials and Chemical Sciences of the U.S. Department of Energy. T.J. acknowledges the support of a NATO grant awarded in 1997.

References and Notes

(1) Cabibil, H.; Kelber, J. A. *Surf. Sci.* **1995**, *329*, 101.
(2) Bartholomew, C. H.; Agrawal, P. K.; Katzer, J. R. *Adv. Catal.* **1982**, *31*, 135.
(3) Menon, P. G. *Chem. Rev.* **1994**, *94*, 1021.
(4) Oudar, J., Wise, H., Eds. *Deactivation and Poisoning of Catalysts*; Marcel Dekker: New York, 1991.
(5) Cox, R. A. *J. Chem. Phys.* **1972**, *76*, 814.
(6) Skotnick, P. A.; Hopkins, A. G.; Brown, C. W. *J. Phys. Chem.* **1975**, *79*, 2450.
(7) Okabe, H. *Photochemistry of Small Molecules*; Wiley: New York, 1978.
(8) Outka, D. A.; Madix, R. J. *Surf. Sci.* **1984**, *137*, 242.
(9) Outka, D. A.; Madix, R. J.; Fisher, G. B.; DiMaggio, G. L. *Langmuir* **1986**, *2*, 406.
(10) Oudar, J. *Catal. Rev.—Sci. Eng.* **1980**, *22*, 171.
(11) Satterfield, C. N. *Heterogeneous Catalysis in Practice*; McGraw-Hill: New York, 1980; p 261.
(12) (a) Ahner, J.; Effendy, A.; Wassmuth, H. W. *Surf. Sci.* **1992**, *269/270*, 372. (b) Ahner, J.; Wassmuth, H. W. *Surf. Sci.* **1993**, *287/288*, 125.
(13) Polčik, M.; Wilde, L.; Haase, J. *Phys. Rev. B* **1998**, *57*, 1868.
(14) Polčik, M.; Wilde, L.; Haase, J.; Brena, B.; Cocco, D.; Comelli, G.; Paolucci, G. *Phys. Rev. B* **1996**, *53*, 13720.
(15) Nakahashi, T.; Hamamatsu, H.; Terada, S.; Sakano, M.; Matsui, F.; Yokoyama, T.; Kitajima, Y.; Ohta, T. *J. Phys. IV* **1997**, *C2*, 679.
(16) Pangher, N.; Wilde, L.; Polčik, M.; Haase, J. *Surf. Sci.* **1997**, *372*, 211.
(17) Nakahashi, T.; Terada, S.; Yokoyama, T.; Hamamatsu, H.; Kitajima, Y.; Sakano, M.; Matsui, F.; Ohta, T. *Surf. Sci.* **1997**, *373*, 1.
(18) Leung, K. T.; Zhang, X. S.; Shirley, D. A. *J. Phys. Chem.* **1989**, *93*, 6164.
(19) Sun, Z. L.; White, J. M. *J. Phys. Chem.* **1994**, *98*, 4641.
(20) Pressley, L. A.; Kiss, J.; White, J. M.; Castro, M. E. *J. Phys. Chem.* **1993**, *97*, 902.
(21) Castro, M. E.; White, J. M. *J. Chem. Phys.* **1991**, *95*, 6057.
(22) Ahner, J.; Effendy, A.; Vajen, K.; Wassmuth, H. W. *Vacuum* **1990**, *41*, 98.
(23) Sosa, A. G.; Walsh, J. F.; Muryn, C. A.; Finetti, P.; Thornton, G.; Robinson, A. W.; D'Addato, S.; Frigo, S. P. *Surf. Sci.* **1996**, *364*, L519.
(24) Solomon, J. L.; Madix, R. J.; Wurth, W.; Stöhr, J. *J. Phys. Chem.* **1991**, *95*, 3687.
(25) Höfer, M.; Stolz, H.; Wassmuth, H. W. *Surf. Sci.* **1993**, *287/288*, 130.
(26) Höfer, M.; Stolz, H.; Wassmuth, H. W. *Surf. Sci.* **1992**, *272*, 342.
(27) Polčik, M.; Wilde, L.; Haase, J.; Brena, B.; Comelli, G.; Paolucci, G. *Surf. Sci.* **1997**, *381*, L568.
(28) Wilson, K.; Hardacre, C.; Baddeley, C. J.; Lüdecke, J.; Woodruff, D. P.; Lambert, R. M. *Surf. Sci.* **1997**, *372*, 279.
(29) Wilson, K.; Hardacre, C.; Lambert, R. M. *J. Phys. Chem.* **1995**, *99*, 13755.
(30) Sun, Y. M.; Sloan, D.; Alberas, D. J.; Kovar, M.; Sun, Z. J.; White, J. M. *Surf. Sci.* **1994**, *319*, 34.
(31) Höfer, M.; Hillig, S.; Wassmuth, H. W. *Vacuum* **1990**, *41*, 102.
(32) Köhler, U.; Wassmuth, H. W. *Surf. Sci.* **1983**, *126*, 448.
(33) Astegger, St.; Bechtold, E. *Surf. Sci.* **1982**, *122*, 491.
(34) Köhler, U.; Wassmuth, H. W. *Surf. Sci.* **1982**, *117*, 668.
(35) Katekaru, J. Y.; Garwood, G. A.; Hershberger, J. F., Jr.; Hubbard, A. T. *Surf. Sci.* **1982**, *121*, 396.
(36) Zebisch, P.; Stichler, M.; Trischberger, P.; Weinelt, M.; Steinrück, H. P. *Surf. Sci.* **1997**, *371*, 235.
(37) Zebisch, P.; Weinelt, M.; Steinrück, H. P. *Surf. Sci.* **1993**, *295*, 295.
(38) Terada, S.; Imanishi, A.; Yokoyama, T.; Takenaka, S.; Kitajima, Y.; Ohta, T. *Surf. Sci.* **1995**, *336*, 55.
(39) Terada, S.; Imanishi, A.; Yokoyama, T.; Kitajima, Y.; Ohta, T. *J. Electron Spectrosc. Relat. Phenom.* **1996**, *80*, 245.
(40) Jackson, G. J.; Lüdecke, J.; Driver, S. M.; Woodruff, D. P.; Jones, R. G.; Chan, A.; Cowie, B. C. C. *Surf. Sci.* **1997**, *389*, 223.
(41) Yokoyama, T.; Terada, S.; Yagi, S.; Imanishi, A.; Takenaka, S.; Kitajima, Y.; Ohta, T. *Surf. Sci.* **1995**, *324*, 25.
(42) Yokoyama, T.; Terada, S.; Imanishi, A.; Kitajima, Y.; Kosugi, N.; Ohta, T. *J. Electron Spectrosc. Relat. Phenom.* **1996**, *80*, 161.
(43) Yokoyama, T.; Imanishi, A.; Terada, S.; Namba, H.; Kitajima, Y.; Ohta, T. *Surf. Sci.* **1995**, *334*, 88.
(44) Burke, M. L.; Madix, R. J. *Surf. Sci.* **1988**, *194*, 223.
(45) Gainey, T. C.; Hopkins, B. J. *J. Phys. C: Solid State Phys.* **1983**, *16*, 975.
(46) Tournas, A. D.; Potts, A. W. *J. Electron Spectrosc. Relat. Phenom.* **1995**, *73*, 231.
(47) Haase, J. *J. Phys.: Condens. Matter* **1997**, *9*, 3647.
(48) Smith, K. E.; Mackay, J. L.; Henrich, V. E. *Phys. Rev. B* **1987**, *35*, 5822.
(49) Onishi, H.; Aruga, T.; Egawa, C.; Iwasawa, Y. *Surf. Sci.* **1988**, *193*, 33.
(50) Smith, K. E.; Henrich, V. E. *Phys. Rev. B* **1985**, *32*, 5384.
(51) Kurtz, R.; Henrich, V. E. *Phys. Rev. B* **1987**, *36*, 3413.
(52) Smith, K. E.; Henrich, V. E. *Surf. Sci.* **1990**, *225*, 47.
(53) Zhang, Z.; Henrich, V. E. *Surf. Sci.* **1994**, *321*, 133.
(54) Li, X.; Henrich, V. E. *Phys. Rev. B* **1993**, *48*, 17486.
(55) Wilson, K.; Lee, A. F.; Hardacre, C.; Lambert, R. M. *J. Phys. Chem. B* **1998**, *102*, 1736.
(56) (a) Dalla Lana, I. G.; Karge, H. G.; George, Z. M. *J. Phys. Chem.* **1993**, *97*, 8005. (b) Yao, H. C.; Stephien, H. K.; Gandhi, H. S. *J. Catal.* **1981**, *67*, 231.
(57) Mitchell, M. B.; Sheinkar, V. N.; White, M. G. *J. Phys. Chem.* **1996**, *100*, 7550.
(58) (a) Pacchioni, G.; Clotet, A.; Ricart, J. M. *Surf. Sci.* **1994**, *315*, 337. (b) Babaeva, M. A.; Tsyganeko, A. A.; Filiminov, V. N. *Kinet. Katal.* **1984**, *25*, 787.
(59) Chaturvedi, S.; Rodriguez, J. A.; Hrbek, J. *J. Phys. Chem. B* **1997**, *101*, 10860.
(60) Chaturvedi, S.; Rodriguez, J. A.; Hrbek, J. *Surf. Sci.* **1997**, *384*, 260.
(61) Rodriguez, J. A.; Hrbek, J. *J. Vac. Sci. Technol., A* **1994**, *12*, 2140.
(62) Rodriguez, J. A.; Kuhn, M.; Hrbek, J. *Chem. Phys. Lett.* **1996**, *251*, 13.
(63) Rodriguez, J. A.; Li, S. Y.; Hrbek, J.; Huang, H. H.; Xu, G.-Q. *J. Phys. Chem.* **1996**, *100*, 14476.
(64) (a) Wagner, C. D.; Riggs, W. M.; Davis, L. E.; Moulder, J. F. *Handbook of X-ray Photoelectron Spectroscopy*; Perkin-Elmer: Eden Prairie, MN, 1978; p 42, 56. (b) Williams, G. P. *Electron Binding Energies of the Elements, Version II*; National Synchrotron Light Source: Brookhaven

National Laboratory, 1992. (c) In ref 55, a difference of 5−5.5 eV is observed between the S 2p binding energies of S and SO_4 on alumina. A separation of ∼5 eV is reported in ref 27 for the S $2p_{3/2}$ binding energies of S and SO_4 on Pt(111), whereas a difference of ∼3 eV is observed between the S $2p_{3/2}$ binding energies of chemisorbed S and SO_2.

(65) Brundle, C. R.; Carley, A. F. *Faraday Discuss. Chem. Soc*. **1975**, *60*, 51.

(66) Rodriguez, J. A.; Jirsak, T.; Chaturvedi, S.; Hrbek, J. *Surf. Sci*. **1998**, *407*, 171.

(67) Stinespring, C. D.; Cook, J. M. *J. Electron Spectrosc. Relat. Phenom*. **1983**, *32*, 113.

(68) Kittel, C. *Introduction to Solid State Physics*, 6th ed.; Wiley: New York, 1986; pp 23, 55.

(69) Dupuis, M.; Chin, S.; Marquez, A. In *Relativistic and Electron Correlation Effects in Molecules and Clusters*; Malli, G. L., Ed.; NATO ASI Series; Plenum: New York, 1992.

(70) Hay, P. J.; Wadt, W. R. *J. Chem. Phys*. **1985**, *82*, 270.

(71) Rodriguez, J. A.; Kuhn, M. *J. Phys. Chem*. **1996**, *100*, 381.

(72) (a) Rodriguez, J. A.; Chaturvedi, S.; Kuhn, M.; Hrbek, J. *J. Phys. Chem. B* **1998**, *102*, 5511. (b) Rodriguez, J. A.; Chaturvedi, S.; Kuhn, M. *Surf. Sci.*, in press.

(73) (a) Mingos, D. M. P. *Transition Met. Chem*. **1978**, *3*, 1. (b) Shenk, W. A. *Angew. Chem., Int. Ed. Engl*. **1987**, *26*, 98.

(74) *Comprehensive Coordination Chemistry*; Wilkinson, G., Gillard, R. D., McCleverty, J. A., Eds.; Pergamon Press: New York, 1987; Chapter 16, 56.

(75) Sellers, H.; Shustorovich, E. *Surf. Sci.* **1996**, *346*, 322.

(76) Sellers, H.; Shustorovich, E. *Surf. Sci.* **1996**, *356*, 209.

(77) Wells, A. F. *Structural Inorganic Chemistry*; Oxford University Press: New York, 1987.

(78) (a) Whitten, J. L.; Yang, H. *Surf. Sci. Rep*. **1996**, *24*, 55 (b) van Santen, R. A.; Neurock, M. *Catal. Rev.—Sci. Eng*. **1995**, *37*, 557 (c) Ruette, F., Ed. *Quantum Chemistry Approaches to Chemisorption and Heterogeneous Catalysis*; Kluwer: Dordtrecht, 1992.

(79) Chase, M. W.; Davies, C. A.; Downey, J. R.; Frurip, D. J.; McDonald, R. A.; Syverud, A. N. JANAF Thermochemical Tables *J. Phys. Chem. Ref. Data* **1985**, *14* (Suppl. 1) 1697.

(80) Egelhoff, W. F. *Surf. Sci. Rep.* **1987**, *6*, 253.

(81) (a) The charges were calculated using a Mulliken population analysis.[81b] As a result of the limitations of this type of analysis,[81c] the charges must be interpreted only in qualitative terms. (b) Mulliken, R. S. *J. Chem. Phys.* **1955**, *23*, 1841. (c) Szabo, A.; Ostlund, N. S. *Modern Quantum Chemistry*; McGraw-Hill: New York.

(82) (a) Rodriguez, J. A.; Campbell, C. T. *J. Phys. Chem.* **1987**, *91*, 6648. (b) Rodriguez, J. A. *Surf. Sci*. **1989**, *222*, 383. (c) Rodriguez, J. A. *Langmuir* **1988**, *4*, 1006. (d) Anderson, A. B.; Nichols, J. A. *J. Am. Chem. Soc*. **1986**, *108*, 4742. (e) Sekine, R.; Adachi, H.; Morimoto, T. *Surf. Sci.* **1989**, *208*, 177.

(83) Abrahams, S. C.; Berstein, J. L. *Acta Crystallogr. B* **1969**, *25*, 1223.

(84) Stevens, W. J.; Basch, H.; Krauss, M. *J. Chem. Phys.* **1984**, *81*, 6026.

(85) Sakaki, S.; Sato, H.; Imai, Y.; Morokuma, K.; Ohkubo, K. *Inorg. Chem.* **1985**, *24*, 4538.

(86) Pacchioni, G.; Clotet, A.; Ricart, J. M. *Surf. Sci.* **1994**, *315*, 337.

(87) Rodriguez, J. A. *Surf. Sci.* **1990**, *226*, 101.

(88) Akhter, S.; Lui, K.; Kung, H. H. *J. Phys. Chem.* **1985**, *89*, 1958.

(89) McKee, M. L. *J. Phys. Chem.* **1996**, *100*, 3473.

(90) Rodriguez, J. A. *Surf. Sci.* **1990**, *230*, 335.

(91) *Lange's Handbook of Chemistry*, 13th ed.; Dean, J. A., Ed.; McGraw-Hill: New York, 1985; Table 9-1.

(92) Jirsak, T.; Rodriguez, J. A.; Chaturvedi, S.; Hrbek, J. *Surf. Sci*., in press.

(93) Sellers, H.; Shustorovich, E. *J. Mol. Catal. A: Chemical* **1997**, *119*, 367.

(94) Chaturvedi, S.; Rodriguez, J. A.; Brito, J. L. *Catal. Lett*. **1998**, *51*, 85.

(95) Lin, J.; May, J. A.; Didzilius, S. V.; Solomon, E. I. *J. Am. Chem. Soc*. **1992**, *114*, 4718.

(96) Rodriguez, J. A.; Kuhn, M. *J. Phys. Chem. B* **1997**, *101*, 3187.